Pure

Syddansk Universitet

Highly specific and selective anti-pS396-tau antibody C10.2 targets seeding-competent tau

Rosenqvist, Nina; Asuni, Ayodeji A; Andersson, Christian R; Christensen, Søren; Daechsel, Justus A; Egebjerg, Jan; Falsig, Jeppe; Helboe, Lone; Jul, Pia; Kartberg, Fredrik; Pedersen, Lars Ø; Sigurdsson, Einar M; Sotty, Florence; Skjødt, Karsten; Stavenhagen, Jeffrey B; Volbracht, Christiane; Pedersen, Jan T

Published in:
Alzheimer's & Dementia: Translational Research & Clinical Interventions

DOI:
10.1016/j.trci.2018.09.005

Publication date:
2018

Document version
Publisher's PDF, also known as Version of record

Document license
CC BY-NC-ND

Citation for pulished version (APA):
Rosenqvist, N., Asuni, A. A., Andersson, C. R., Christensen, S., Daechsel, J. A., Egebjerg, J., ... Pedersen, J. T. (2018). Highly specific and selective anti-pS396-tau antibody C10.2 targets seeding-competent tau. Alzheimer's & Dementia: Translational Research & Clinical Interventions, 4, 521-534. DOI: 10.1016/j.trci.2018.09.005

General rights
Copyright and moral rights for the publications made accessible in the public portal are retained by the authors and/or other copyright owners and it is a condition of accessing publications that users recognise and abide by the legal requirements associated with these rights.

- Users may download and print one copy of any publication from the public portal for the purpose of private study or research.
- You may not further distribute the material or use it for any profit-making activity or commercial gain
- You may freely distribute the URL identifying the publication in the public portal ?

Take down policy
If you believe that this document breaches copyright please contact us providing details, and we will remove access to the work immediately and investigate your claim.

Download date: 15. Nov. 2018

Alzheimer's & Dementia: Translational Research & Clinical Interventions 4 (2018) 521-534

Featured Article

Highly specific and selective anti-pS396-tau antibody C10.2 targets seeding-competent tau

Nina Rosenqvist[a], Ayodeji A. Asuni[a], Christian R. Andersson[a], Søren Christensen[a], Justus A. Daechsel[a], Jan Egebjerg[a], Jeppe Falsig[a], Lone Helboe[a], Pia Jul[a], Fredrik Kartberg[a], Lars Ø. Pedersen[a], Einar M. Sigurdsson[b,c], Florence Sotty[a], Karsten Skjødt[d], Jeffrey B. Stavenhagen[e], Christiane Volbracht[a], Jan T. Pedersen[a,*]

[a]*H. Lundbeck A/S, Valby, Denmark*
[b]*Department of Neuroscience and Physiology, New York University School of Medicine, New York, NY, USA*
[c]*Department of Psychiatry, New York University School of Medicine, New York, NY, USA*
[d]*Department of Cancer and Inflammarion Research, University of Southern Denmark, Odense C, Denmark*
[e]*Therachon AG, Basel, Switzerland*

Abstract

Introduction: The abnormal hyperphosphorylation of the microtubule-associated protein tau plays a crucial role in neurodegeneration in Alzheimer's disease (AD) and other tauopathies.
Methods: Highly specific and selective anti-pS396-tau antibodies have been generated using peptide immunization with screening against pathologic hyperphosphorylated tau from rTg4510 mouse and AD brains and selection in in vitro and in vivo tau seeding assays.
Results: The antibody C10.2 bound specifically to pS396-tau with an IC_{50} of 104 pM and detected preferentially hyperphosphorylated tau aggregates from AD brain with an IC_{50} of 1.2 nM. C10.2 significantly reduced tau seeding of P301L human tau in HEK293 cells, murine cortical neurons, and mice. AD brain extracts depleted with C10.2 were not able to seed tau in vitro and in vivo, demonstrating that C10.2 specifically recognized pathologic seeding-competent tau.
Discussion: Targeting pS396-tau with an antibody like C10.2 may provide therapeutic benefit in AD and other tauopathies.
© 2018 The Authors. Published by Elsevier Inc. on behalf of the Alzheimer's Association. This is an open access article under the CC BY-NC-ND license (http://creativecommons.org/licenses/by-nc-nd/4.0/).

Keywords: Anti-tau antibodies; Phospho-serine 396; Tau seeding; Monoclonal antibody; C10.2; D1.2; C5.2; C8.3

1. Introduction

Microtubule-associated protein tau deposited as straight and paired helical filaments (PHFs) form the neurofibrillary tangles (NFTs), one of the hallmarks of Alzheimer's disease (AD) [1]. These tau aggregates are detergent-insoluble and contain predominantly hyperphosphorylated tau [2]. The longest isoform of tau (2N4R or Tau-441) contains 85 putative phosphorylation sites (Ser, Thr, or Tyr) and of these, half have been confirmed experimentally [3]. Phosphorylation sites are located mainly around the microtubule binding (MTB) domains, and tau is dynamically phosphorylated and dephosphorylated by several kinases and phosphatases. Tau associates with microtubules in its dephosphorylated form, thereby acting as a stabilizer regulating axonal transport [3]. Under normal conditions, cytosolic tau contains, on average, two to three phosphorylated sites [4]. In paired helical and straight filamentous material tau is hyperphosphorylated, with at least seven sites phosphorylated [4,5]. Braak and Braak [6] and Nelson et al. [7] demonstrated that the spatiotemporal appearance of NFTs closely follows the development of neurodegeneration and clinical

*Corresponding author. Tel.: +45 30832887; Fax: +45 36438258.
E-mail address: jatp@lundbeck.com

https://doi.org/10.1016/j.trci.2018.09.005
2352-8737/ © 2018 The Authors. Published by Elsevier Inc. on behalf of the Alzheimer's Association. This is an open access article under the CC BY-NC-ND license (http://creativecommons.org/licenses/by-nc-nd/4.0/).

progression of AD. Ghost tangles, presumably remnants from dead neurons, appear in more advanced stages of AD [8]. The spatiotemporal spreading of tau pathology suggests that tau itself may form an endopathogen species, which propagates pathology from one neuron to adjacent cells. Clavaguera et al. [9] demonstrated that aggregated hyperphosphorylated tau isolated from transgenic mouse brains acts as a mediator of tau seeding and on hippocampal injection induces tau pathology in transgenic mice (ALZ17) otherwise lacking tau aggregates. Also, peripheral injection of brain extracts from old tau transgenic mice increased tangle pathology [10]. Recent biochemical and in vivo seeding studies demonstrated that small tau fibrils likely are the main seeding and propagating species [11–13]. Furthermore, cryo-electron microscopy [14] studies have demonstrated that a cross-β/β-helix structure covering residues 306 to 378 constitutes a tau aggregate core and may be the seeding competent species for propagation of tau pathology in AD and other tauopathies. Thus, seeding-competent pathologic tau species could represent a viable therapeutic target. Active vaccination studies with tau peptides indicated that raising an immune response against specific phosphorylated epitopes of tau could prevent the formation of tau pathology in tau transgenic mouse models [15–20]. Subsequently, passive immunization with different phospho-dependent and phospho-independent tau antibodies was reported to reduce tau pathology in different tau transgenic mouse models [21–31]. In this report, we describe the generation of pS396-tau specific antibodies and demonstrate in vitro and in vivo evidence that suggest anti-pS396 antibodies have a therapeutic potential to prevent seeding of tau pathology.

2. Materials and methods

2.1. Generation of antibodies

Male and female mice (C57BL/6 and FVB strains) were immunized with peptide P30-pS396/pS404-tau; containing the P30 (tetanus toxin P30 helper peptide epitope, FNNFTVSFWLRVPKVSASHLEGPSL) and phosphorylated tau (386–408) peptide corresponding to the sequence P30-[TDHGAEIVYK(pS)PVVSGDT(pS)PRHL] (US patent, US2008050383). P30-pS396/pS404-tau was formulated in TiterMax Gold Adjuvant from Sigma-Aldrich (400 μg/mL peptide mixed 1:1 vol/vol) following the manufacturer's protocol, and 20 μg peptide antigen (100 μL) was injected subcutaneously. All peptide-immunized mice were boosted with 0.5 μg P30-pS396/pS404-tau/TiterMax four times at monthly intervals. The mice were finally boosted with 0.5 μg P30-pS396/pS404-tau (without TiterMax) 3 days before fusion of splenocytes with SP-2 cells. Hybridomas exhibiting positive binding to enzyme-linked immunosorbent assay plates (Nunc Maxisorp) coated with 1 μg/mL pS396/pS404-tau in coating buffer (carbonate buffer, pH 9.4) were selected for recloning. By this procedure, three clones were generated (C10.2, C10.1 from C57/BL6, and D1.2 from FVB mice) and characterized in subsequent range of assays. In addition, the following antibodies were included: PHF13 (tau-p396, Thermo Fisher Scientific); AT8 (tau-p202/p205, Thermo Fisher Scientific); Tau 5 (total tau, Thermo Fisher Scientific); E1 (human-specific tau (19–33), generated in rabbit [32].

2.2. Analysis of peptide binding

2.2.1. Peptide competition binding assay

Meso Scale discovery (MSD) plates were coated overnight at 4°C with 100 ng/mL of peptide tau (386–408)-pS396/pS404 in coating buffer, blocked for 1 hour at 25°C, and washed three times (0.1% bovine serum albumin [fraction V], 0.1% NP40 in phosphate buffered saline (PBS), pH 7.4). Low concentrations of tau-pS396–specific antibodies (typically $0.1 \times K_d$, e.g., 1–2 ng/mL or lower to avoid ligand depletion) were incubated 1:1 with graded concentrations (1 hour at 22°C) of tau (386–408)-pS396/pS404, followed by washing three times and finally subjected to analysis of unbound antibody in tau (386–408)-pS396/pS404–coated MSD plates. Antibody binding in wells was detected using MSD Sulfotag goat anti-mouse immunoglobulin G (IgG) antibody (catalog no R32AC-1) at 1:500 dilution. Inhibition curves and IC_{50} values were obtained by fitting to one site binding models using GraphPad Prism software. One hundred nanometers of tau (386–408)-pS396, tau (386–408)-pS404, tau (260–270)-pS262, or nonphosphorylated tau (386–408) were tested for inhibition of antibody binding in parallel and compared with tau (386–408)-pS396/pS404 inhibition curve.

2.2.2. Surface plasmon resonance Biacore analysis

The antibodies were tested for binding to monophosphorylated tau (386–408)-pS396 and double phosphorylated pS396/pS404-tau peptides. Nonphosphorylated tau (386–408) was used as nonbinding peptide control. Antibodies were captured on CM5 sensor chips coated with anti-mouse IgG antibody (GE catalog no BR100838). The tau peptides were initially screened for binding at their top concentrations. Subsequently, peptides demonstrating binding were titrated into the captured antibodies. The titration was performed twice. For each antibody and peptide interaction, the sensorgrams were fit globally to a simulated 1 to 1 kinetics binding model using the BiaEvaluation software (estimated kon, koff, and K_d from the fit are reported in Table 1).

2.3. Mouse tissue

The rTg4510 transgenic mice express human 4-repeat mutant P301L tau [33]. The mouse colony was bred and housed as described earlier [34]. Single-transgenic tTA

Table 1
SPR Biacore peptide binding

Antibody	Tau 386–408 peptide	Peptide MW (Da)	Average of expected R_{max} (RU)	Average of R_{max} (RU)	Average kon (1/ms)	SD_kon (1/ms)	Average koff (1/s)	SD_koff (1/s)	K_d (nM)	SD K_d (nM)	Average stoichiometry
D1.2	pS396	2560	9	10	2.3×10^6	2.8×10^4	2.4×10^{-2}	10^{-4}	11	0.1	1.0
	pS396/pS404	2624	10	10	1.7×10^6	7.1×10^3	2.6×10^{-2}	10^{-3}	15	0.6	1.0
C10.2	pS396	2560	6	8	2.8×10^6	1.6×10^5	7.4×10^{-2}	7×10^{-3}	27	1.3	1.3
	pS396/pS404	2624	7	8	2.2×10^6	2.7×10^5	6.7×10^{-2}	10^{-4}	31	3.8	1.2

Abbreviations: SD, standard deviation; SPR, surface plasmon resonance.
On (kon) and off (koff) rates and K_d were determined. The K_d for the pS396 peptide is virtually identical to that for the diphosphorylated peptide pS396/pS404 indicating clear specificity for pS396.

mice without human tau expression served as negative control subjects. All animal experiments were performed in accordance with the European Communities Council Directive no. 86/609, the directives of the Danish National Committee on Animal Research Ethics, and Danish legislation on experimental animals (license no. 2014-15-0201-00339). Mice were euthanized by cervical dislocation, the brains were quickly removed and parted from the cerebellum and hind brain. The forebrain containing the cerebral cortex and hippocampus was snap-frozen on dry ice and stored at −80°C until use. For in vitro and in vivo seeding material, we used pooled brains from rTg4510 or tTA mice aged 36 to 40 weeks when tau pathology was advanced in the forebrain.

2.4. Human tissue

Frozen samples of frontal cortices from AD and healthy control (HC) cases were acquired from Tissue Solutions (United Kingdom). Gray matter tissue was isolated and pooled from two (seeding) or four (dot blot) AD and four HC cases. Subject characterization can be found in Supplementary Table 1.

2.5. Tissue extraction and fractionation

The soluble S1 and insoluble P3 preparations were performed as described earlier [35]. Tau fractions used as seeds in vitro were prepared from rTg4510 forebrains omitting protease and phosphatase inhibitors and ion chelators in the buffers. For solution phase binding, P3 fractions were prepared from AD frontal cortices. For in vivo seeding, crude extracts were prepared from rTg4510 and tTA littermate mice and from human AD and HC cortical tissue as described by Clavaguera et al. [9].

2.6. Solution phase antibody binding to AD P3 material and recombinant phosphorylated tau-441

MSD plates were coated overnight at 4°C with 0.5 μg/mL C10.2 (capture antibody) in coating buffer, blocked for 1 hour at 25°C, and washed three times. P3 fraction from AD cortex diluted 1:1000 (2–4 μg/mL total protein) or 30 ng/mL recombinant phosphorylated tau (SignalChem, tau-441 glycogen synthase kinase 3 beta-phosphorylated (T08-50FN)) and graded concentrations (0–300 nM) of C10.2, D1.2, PHF13, and C10.1 (negative control), respectively, were incubated for 1 hour at 22°C followed by washing three times. C10.2-captured tau was detected using a 1:50 diluted anti-tau antibody (Sulfotag goat anti-total tau antibody, MSD catalog no R32AC-1).

2.7. Dot blot

One microliter of samples S1 and P3 isolated from AD and HC cortices or from rTg4510 and tTA brains were applied to nitrocellulose membranes. After blocking with 5% nonfat milk and 0.1% Triton X-100 in Tris-buffered saline, the membranes were incubated with 1 μg/mL D1.2 or C10.2. Membranes were washed and incubated with peroxidase-conjugated anti-mouse antibody (1:5000; Jackson ImmunoResearch). Bound antibodies were detected using an enhanced chemiluminescence system (ECL PLUS kit; Perkin Elmer).

2.8. Immunohistochemistry on human brain sections

Formalin-fixed paraffin-embedded frontal cortex from three AD (Braak stage V–VI) and three age-matched HC cases were acquired from tissue solutions. Subject characterization can be found in Supplementary Table 1. Four-micrometer sections were deparaffinized, rehydrated, and subjected to antigen retrieval by boiling in 10 mM citrate buffer, pH 6. The sections were incubated overnight at 4°C with C10.2, D1.2, or C10.1 antibodies at 1 μg/mL. After thorough rinsing, sections were incubated with biotinylated anti-mouse antibodies (Dako). Immunoreactivity was visualized using the avidin-biotin complex (Vector) and 0.05% 3,3′-diaminobenzidine. Sections were counterstained with hematoxylin.

2.9. Immunodepletion for seeding

One hundred micrograms of antibody was immobilized to 500 μL of magnetic Dynabead suspension (Immunoprecipitation Kit Dynabeads Protein G Novex, catalog no 10007D). After thorough washing, the beads were mixed with 100 μL crude extract of rTg4510 or AD frontal cortex

(3–5 mg/mL total protein). Mixtures were incubated at room temperature for 10 minutes. The magnetic beads were separated from the extract, and extracts were aliquoted, snap frozen, and stored at −80°C until use.

2.10. Primary neuronal culture

Cortical cultures (CTXs) were isolated from day 14 to 16 tTA or rTg4510 mouse embryos as described previously [36]. Embryos were genotyped using primer pairs as described [33]. Neurons were cultured in glia-conditioned neurobasal medium supplemented with 2% B-27 supplement with antioxidants, 0.5 mM L-glutamine, 100 U/mL penicillin, 0.1 mg/mL streptomycin (all solutions from Gibco-BRL Invitrogen) and treated with 1 μM cytosine arabinoside at days in vitro (DIV) 4 to halt proliferating cells. The proportion of glia cells in the cultures was less than 10%, as assessed by an antibody against glia-fibrillary-acidic protein at DIV7.

2.11. Tau and antibody uptake in tTA neurons

At DIV7, CTXs isolated from tTA mouse embryos were treated with a mixture of 2 ng human tau from rTg4510 P3 fractions and 10 μg antibodies (D1.2, C10.2, C10.1, and mouse IgG control) or PBS. The tau seed/antibody mixture was preincubated for 2 hours at 4°C before adding to CTX. After 24 hours, the cells were washed, fixed in 3.7% formaldehyde, and immunostained for human tau using the E1 antibody and for mouse immunoglobulins with anti-mouse IgG antibody conjugated with Alexa Fluor 546 (Molecular Probes). Anti-rabbit IgG conjugated with Alexa Fluor 488 (Molecular Probes) was used as the secondary antibody to detect the E1 signal. Nuclei were counterstained with Hoechst 33342. Human tau and antibody uptake was detected by image processing software using a spot-detection algorithm on the charge-coupled device camera-based ArrayScan VTI HCS system (Cellomics Scan software version 6.5). Twenty microscopic fields were analyzed per well and data quantified as spots per cell.

2.12. Tau seeding in rTg4510 neurons

At DIV7, CTXs isolated from rTg4510 mouse embryos were treated with a mixture of 0.2 ng human tau from rTg4510 P3 fractions and 10 μg antibodies (D1.2, C10.2, C10.1, and mouse IgG control) or PBS. The tau seed/antibody mixture was preincubated for 2 hours at 4°C before adding to CTX. At DIV11, a complete medium change was performed to remove any residual tau and antibody. At DIV15, neurons were lysed in ice-cold lysis buffer (1% Triton X-100 in 50 mM Tris, 150 mM NaCl (pH 7.6) with 1% protease inhibitor mixture [Roche], 1% phosphatase inhibitor cocktail I and II [Sigma], and 0.2% Benzonase [Sigma]) under shaking at 200 rpm for 45 minutes at 4°C. Lysates were used in the Cisbio tau aggregation and bicinchoninic acid assays according to manufactures' instructions.

For detection of cell viability after P3 and antibody addition, the percentage of viable cells in the neuronal cultures was quantified at DIV15 from parallel plates by their capacity to reduce 3-(4,5-dimethylthiazol-2-yl)-2,5-diphenyltetrazolium bromide (MTT) after incubation with 0.5 mg/mL MTT for 60 minutes.

2.13. In vivo seeding

To establish a window for detection of seeding-induced tau pathology in the rTg4510 model the development of tau phosphorylation and tangle formation was delayed by suppressing tau transgene expression with doxycycline (as described in Refs. [33,34]). We established that the presence of doxycycline from conception until the age of 3 weeks delayed tau phosphorylation in hippocampus at age from 16 weeks until around 24 weeks, thus providing enough time for seeding-induced tau pathology to develop before interference from endogenous tau pathology.

Seeding: doxycycline-treated rTg4510 and tTA mice were seeded at the age of 10 weeks as follows: mice were anesthetized by isoflurane inhalation and fixed in a stereotactic frame. The dural surface was carefully exposed and 2 μL crude extracts prepared from rTg4510, tTa, AD, or HC brains were slowly infused (1 μL/min) using a 10 μL syringe with a 26 gauche, beveled tip into the right hippocampus at the following coordinates: M/L, −2.0; A/P, −2.4; V, −1.4 from bregma and the dural surface. The wound was closed and sealed with sutures and mice were homeothermally supported during recovery from anesthesia. Mice were then housed for 4 to 12 weeks before being perfusion-fixed with 4% paraformaldehyde.

Antibody treatment and blood sampling: antibodies (C10.2, D1.2, or control mouse IgG) were prepared in a concentration of 1.5 mg/mL in sterile PBS. At age from 8 weeks (2 weeks before seeding with rTg4510 or tTA crude extracts) until euthanization at 22 weeks the mice received one weekly intraperitoneal (ip) dose of antibody (15 mg/kg). Blood samples were drawn every 2 to 4 weeks and the concentration of antibody in plasma was analyzed by enzyme-linked immunosorbent assay using a phosphorylated tau peptide (386–408, pS396/pS404 from TAG, Denmark) as capture and a Sulfotag goat anti-mouse antibody for detection (MSD catalog no R32AC-1). In a seeding experiment comparing three different dosing paradigms, C10.2 antibodies (15 mg/kg, ip) were dosed once weekly at age from 8 to 22 weeks (full), once weekly at age from 14 to 22 weeks (post), or once weekly at age from 8 to 10 weeks (pre). A control mouse IgG was dosed once weekly at age from 8 to 22 weeks. All mice were seeded with AD crude extract at the age of 10 weeks and perfusion-fixed with 4% paraformaldehyde at the age of 22 weeks.

2.14. Histology on seeded mouse brains

Perfusion-fixed brains were processed at Neuroscience Associates (Knoxville, TN) using MultiBrain technology. Up to 25 mouse brains were embedded together and freeze-sectioned at 35 μm in the coronal plane through the entire brain. Every sixth section was subjected to AT8 immunohistochemistry to reveal phosphorylated tau, and every sixth section was stained with the Gallyas silver stain to reveal NFT. Gallyas silver and AT8 positive neurons (soma) were counted in ipsilateral and contralateral sides of the hippocampus of all brains. All subregions of the hippocampus were included, omitting the subiculum. Eight sections covering the dorsal and ventral hippocampus were counted per brain (equivalent to A/P, −1.22 to −2.8 from bregma). Results reflect the sum of positive neurons accumulated over the eight sections. The Gallyas pathology was quantified in the entorhinal cortex on the six most caudal sections containing cerebral cortex. The ImageJ program was used for quantification. Group variance was analyzed using Bartlett's test of equal variance. Because there was a significant difference in variance between groups the nonparametric Kruskal-Wallis test was used, followed by Dunn's multiple comparison test.

3. Results

3.1. Generation and characterization of tau pS396 and pS404 antibodies

3.1.1. Selection of clones

Mouse monoclonal antibodies were generated (Fig. 1) by immunization with P30-pS396/pS404-tau peptide, and 150 clones were initially selected based on binding activity to the pS396/pS404-tau peptide. Subsequently, the panel of

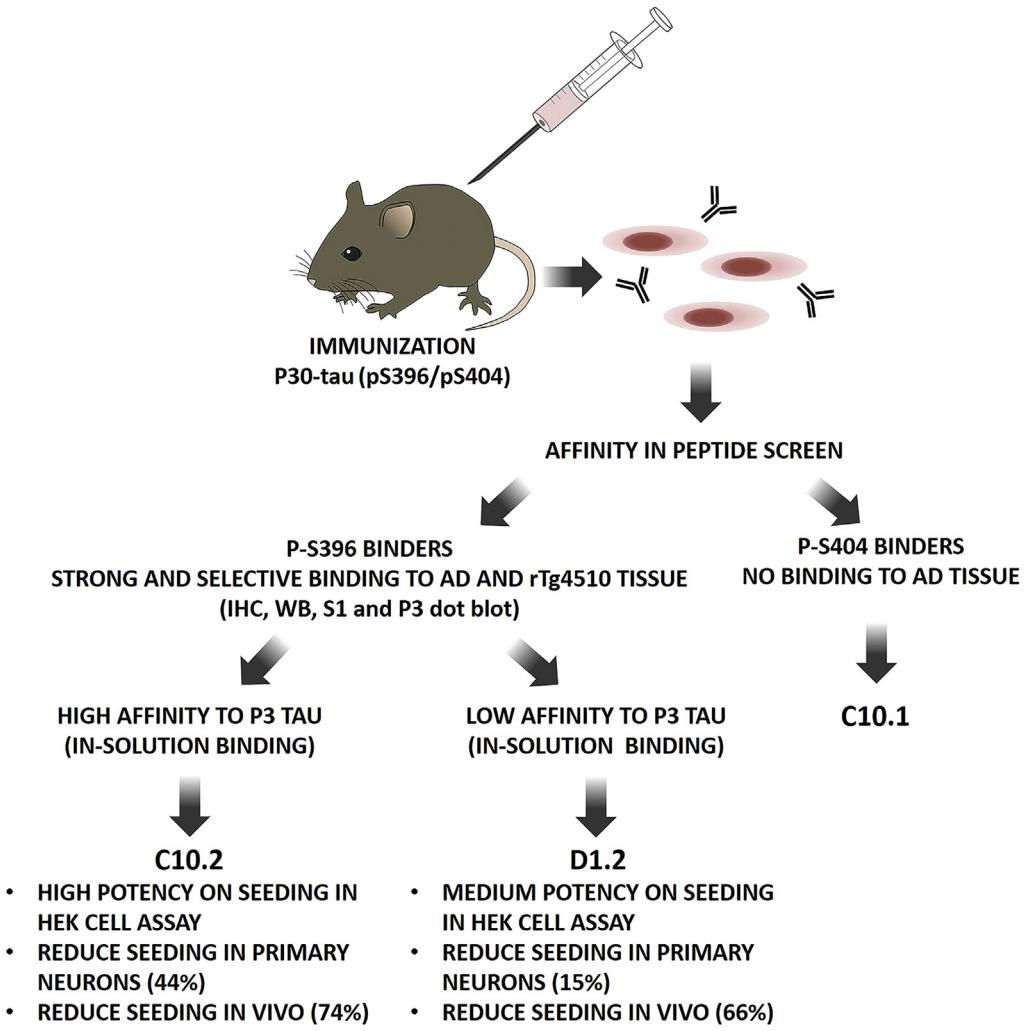

Fig. 1. Screening cascade and summary over the characterization of the phospho-tau antibodies described in this article. Abbreviations: AD, Alzheimer's disease; IHC, immunohistochemistry; P3, sarkosyl-insoluble brain fraction; S1, soluble brain fraction; WB, Western blot.

clones was reduced to four based on potent binding to peptide tau (p396 epitope only), full-length in vitro phosphorylated tau, and AD tissue. Sequencing revealed three of these antibodies (C10.2, C5.2, and C8.3) to have nearly identical complementarity determining region leaving C10.2 (IgG1κ) and D1.2 (IgG2κ) from a different series for further characterization. From the same immunizations, C10.1 (IgG1κ) was selected based on pS404-tau binding. The apparent affinities (IC_{50}) of the antibodies to the pS396/pS404-tau peptide were determined in a competition binding assay for D1.2 (19 nM), C10.2 (66 nM), and C10.1 (24 nM) (Supplementary Fig. 1A).

3.1.2. Antibody specificity and selectivity

Antibody specificity toward S396 and S404 phosphorylation sites was assessed by the ability of monophosphorylated peptides to compete with antibody binding to pS396/pS404-tau. Both D1.2 and C10.2 bindings were inhibited by the tau peptide phosphorylated at S396 but not when monophosphorylated at S404, whereas competition of C10.1 binding requires phosphorylation of S404 but not of S396 (Fig. 2A). The antibodies were further characterized for their ability to bind the soluble S1 or sarkosyl-insoluble P3 tau fractions obtained from AD and HC brains or from rTg4510 and tTA control brains by dot blot analysis. Both

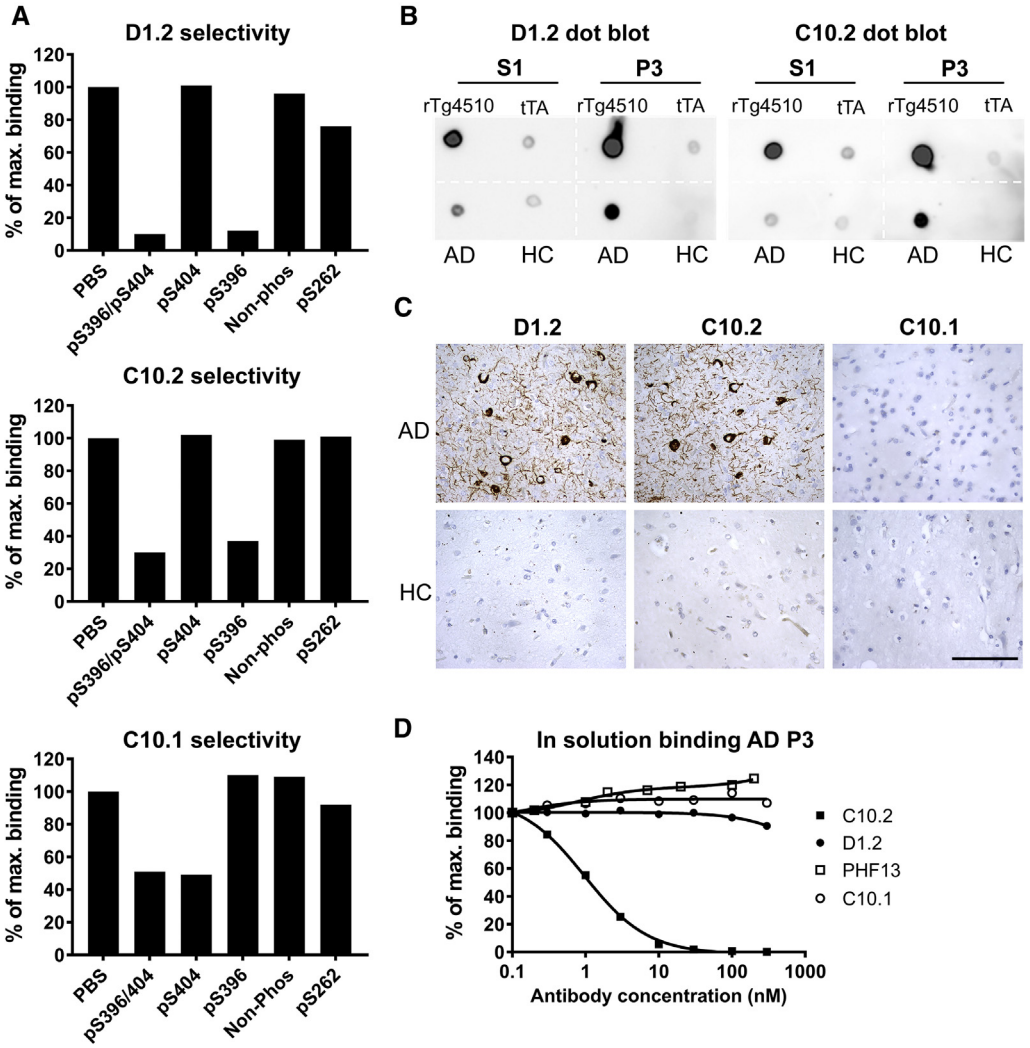

Fig. 2. Antibody selectivity toward pS396 or pS404 tau (386–408) peptides and disease material. (A) Antibodies were mixed with the indicated peptides and screened for binding on tau (386–408)-pS396/pS404–coated MSD plates. Data presented as percentage binding in relation to PBS control incubation. Both D1.2 and C10.2 bind to tau phosphorylated at S396 but not to nonphosphorylated or S404-phosphorylated tau, whereas C10.1 requires phosphorylation of S404 for binding but not S396. (B) Dot blot demonstrating selective binding by D1.2 and C10.2 to soluble (S1) and sarkosyl-insoluble (P3) fractions isolated from rTg4510 and AD brains compared with tTA littermates and HC brain fractions. (C) Immunohistochemical staining of AD and HC brain sections of frontal cortex. Photomicrographs are representative of three AD and three HC cases, images from a single AD and a single HC case are shown. Scale bar: 50 μm. (D) In-solution binding of antibodies to AD brain. Insoluble P3 tau fraction was mixed with antibodies D1.2, C10.2, C10.1, or PHF13 before binding to C10.2-coated MSD plates. Data are presented as percent P3 binding when preincubated with increasing amounts of antibody in relation to P3 binding without added antibody. At the given antibody concentrations, only C10.2 resulted in a concentration-dependent decrease in binding. Abbreviations: AD, Alzheimer's disease; HC, healthy control; MSD, Meso Scale discovery; PBS, phosphate buffered saline.

D1.2 and C10.2 strongly bind P3 material from AD and rTg4510 brains and S1 from rTg4510 mice (Fig. 2B). This is in line with antibodies D1.2 and C10.2 binding preferentially to hyperphosphorylated tau from human AD brain or rTg4510 mouse brains demonstrated by Western blot (Supplementary Fig. 2). C10.1 only binds normal phosphorylated tau protein in the S1 fractions (Supplementary Fig. 2). By immunohistochemistry, NFTs, neuropil threads, and dystrophic neurites were detected in AD brain sections by the D1.2 and C10.2 antibodies (Fig. 2C). No immunoreactivity was detected in HC sections. In contrast, C10.1 did not stain AD sections. In subsequent assays, C10.1 served as negative control.

3.1.3. Antibody affinity to tau peptides

Antibodies D1.2 and C10.2 were subjected to detailed binding kinetics analysis using surface plasmon resonance binding on the Biacore system (Table 1). D1.2 and C10.2 bind the tau (386–408)-pS396 with an affinity (K_d) of 11 and 27 nM, respectively. In agreement with surface plasmon resonance, MSD-based analysis showed that D1.2 and C10.2 bind equally well to diphosphorylated peptides as well as to monophosphorylated S396 (Fig. 2A). Both antibodies showed similar binding to pS396-tau peptide.

We developed an inhibition binding assay using sarkosyl-insoluble P3 tau isolated from AD brains in the solution phase, based on the hypothesis that P3 material contains tau in a seeding competent conformation and the solution phase mimics the extracellular conditions. Antibody binding potency toward the P3 AD fractions was assessed using an inhibition assay with MSD plates coated with C10.2. We have compared C10.2 and D1.2 with PHF13 and demonstrated that only C10.2 showed potent inhibition, with an IC_{50} of 1.2 nM. As expected, the C10.1 was not able to compete the antigen capture in C10.2 plates in the solution phase (Fig. 2D), because C10.1 did not bind to hyperphosphorylated tau in the P3 fraction (Supplementary Fig. 2C). This contrasts with antibody competition using in vitro phosphorylated tau-441 for antigen capture in C10.2-coated plates where D1.2 (IC_{50}; 50 pM), C10.2 (IC_{50}; 104 pM), and PHF13 (IC_{50}; 758 pM) all compete with binding to C10.2 (Supplementary Fig. 1B).

3.1.4. Immunodepletion of phosphorylated tau from rTg4510 and AD brain extracts

To investigate whether hyperphosphorylated or normal tau is recognized by C10.2 and D1.2, crude extracts prepared from rTg4510 and tTA mouse brains were immunodepleted by either of the antibodies, and the residual extract was examined by Western blot. Both antibodies reduced the amount of pS396 tau recognized by C10.2 by approximately 85%. There was a minor effect on the total tau levels (detected by E1) where only the hyperphosphorylation-specific 64 kDa band was markedly reduced (Supplementary Fig. 3A).

The two antibodies were also tested for their ability to remove tau species from AD and HC crude extracts. Both D1.2 and C10.2 removed most pS396 tau recognized by C10.2 (approximately 90% of the Western blot signal), including the typical pS396-positive AD smear (Supplementary Fig. 3B). However, although depletion with C10.2 efficiently removes the two distinct hyperphosphorylated tau bands (64 and 69 kDa), D1.2 left some residual 64 and 69 kDa tau being recognized by C10.2. Overall, the depletion of hyperphosphorylated AD tau species using D1.2 and C10.2 only resulted in a small reduction in the total pool of tau (Supplementary Fig. 3B). The immunodepleted rTg4510 and AD brain extracts were subsequently used in seeding experiments.

Collectively, our data demonstrate that although all three antibodies bind peptide tau and full-length phosphorylated tau, binding to AD and rTg4510 hyperphosphorylated tau can only be achieved by C10.2 and D1.2 directed toward pS396-tau and not by the pS404-tau specific C10.1. Furthermore, C10.2 proved to be superior to D1.2 in binding hyperphosphorylated tau in solution phase assay.

3.2. Evaluation of C10.2, D1.2, and C10.1 effects on in vitro seeding

3.2.1. Tau seeding assay in HEK293 cells

We established an HEK cell–based seeding assay by transiently overexpressing 0N4R-P301L human tau. In this assay, tau aggregation was assessed either by an aggregation-specific immunoassay or by Western blot analysis of the Triton X-100 insoluble tau, 3 days after adding rTg4510 hard spin crude extracts (Supplementary methods). The assay was used to measure the effects of C10.2 immunodepletion on the seeding capacity of rTg4510 extract. C10.2 immunodepletion resulted in 88% reduction in aggregated tau (measured in Cisbio assay) and 97% reduction in the pS396-positive insoluble tau (measured by Western blot) (Supplementary Fig. 4A).

Next, we generated a stable HEK cell line expressing the MTB repeats of human tau with P301L/V337M mutations fused to green fluorescent protein and measured seeding as fluorescent inclusion bodies on induction with rTg4510 seeds (Supplementary methods). Preincubation of the seeding material (rTg4510 hard spin crude extract) with antibodies D1.2 or C10.2 results in a concentration-dependent prevention of seeding (Supplementary Fig. 4B). The maximum inhibition achieved at the highest antibody concentration applied (100 nM) was 86% for C10.2 and 35% for D1.2 with calculated IC_{50} value of 4 nM for C10.2. We also demonstrated that the effect of the C10.2 antibody can be abolished by incubating the antibody with the tau (pS396/pS404) peptide before adding it to the seeds and cells (Supplementary Fig. 4C). As expected, C10.1 did not modulate tau seeding in vitro.

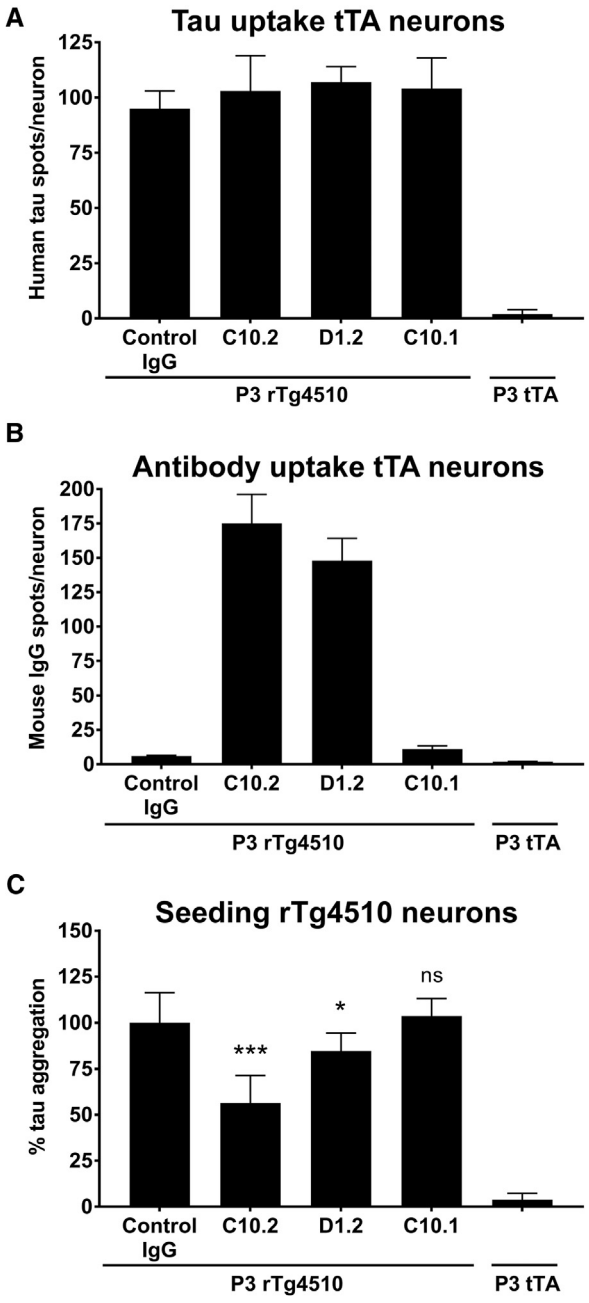

Fig. 3. C10.2 and D1.2 reduce tau seeding in rTg4510 cortical neuronal cultures without blocking the uptake of seeds into neurons. (A) Uptake of human tau from rTg4510 P3 material was measured in tTA control neurons not expressing human tau. The uptake was measured as spots inside the cells detected by the human tau-specific E1 antibody. Preincubation of P3 material with C10.2, D1.2, or C10.1 does not prevent tau seed uptake. (B) In the same experiment, the uptake of antibodies was detected by anti-mouse IgG and measured as positive spots inside the neuronal cell bodies. Data in A and B are presented as the mean ± SD and represents quantifications from three wells with 20 fields/well analyzed. (C) Tau seeding was analyzed with the Cisbio tau aggregation assay in rTg4510 neuron cultures. Before addition of rTg4510 P3 seeding material to the neurons, it was preincubated with C10.2, D1.2, C10.1, or control mouse IgG. An equal volume of P3 isolated from tTA controls was added to the neuronal cultures as negative control not inducing tau seeding. Neurons seeded at DIV7, medium changed at DIV11, and cells lysed at DIV15. Data are presented as percentage aggregation normalized to total protein in relation to IgG control, mean ± SD from 5 to 15 wells from 2 to 4 independent experiments. One way ANOVA Newman-Keuls multiple comparison test, $*P < .05$; $***P < .001$; $n = 10–60$. Abbreviations: ANOVA, analysis of variance; DIV, days in vitro; IgG, immunoglobulin G; SD, standard deviation.

3.2.2. Seeding assay in cultured primary cortical neurons

To further investigate how the tau antibodies interfere with the seeding process we analyzed the uptake of antibody and human tau from rTg4510 P3 fractions in tTA neurons expressing only endogenous murine tau. In line with previous reports [12,31], human tau from P3 was taken up by the neurons within 24 hours (Fig. 3A). The tau uptake was not affected by the presence of tau antibodies (Fig. 3A) and immunofluorescent detection revealed that both C10.2 and D1.2 antibodies were detected inside the neurons (Fig. 3B), whereas C10.1 was not detected in line with lack of binding to hyperphosphorylated tau from the P3 fraction (Supplementary Fig. 2C). Neither was the control IgG detected in the neurons. These results suggest that only pS396-tau antibodies binding to hyperphosphorylated tau in the P3 fraction were taken up together with P3 tau by the neurons.

Next, we investigated whether hyperphosphorylated tau from the P3 rTg4510 fraction can induce tau seeding in rTg4510 neuron cultures. These cortical neurons show the expression of the 4R0N human tau isoform with P301L mutation in addition to murine tau (data not shown) and no hyperphosphorylated/aggregated tau was detected in neurons cultured up to 4 weeks (data not shown). When neurons were incubated with low concentrations of fibrillary tau species (2 pg/μL) from the rTg4510 P3 fraction, aggregated tau was observed by the Cisbio assay 8 days after the seeding (Fig. 3C). Tau seeding did not result in impaired viability of the neuronal cultures measured by MTT reduction test (data not shown). When preincubating the P3 fraction with C10.2 or D1.2 before adding to the neurons, the tau aggregation was reduced approximately 50% and 15%, respectively (Fig. 3C). The preincubation with C10.1 did not prevent tau aggregation in the neurons (Fig. 3C).

3.3. Evaluation of C10.2 and D1.2 effects in in vivo seeding

3.3.1. Establishment of the rTg4510 mouse seeding model

We seeded tau pathology in vivo in short-term doxycycline-treated rTg4510 mice [34]. Without juvenile doxycycline treatment, tau pathology develops at an early age (10–16 weeks) [34]. By a transient doxycycline treatment at age from conception to 3 weeks the tau pathology was delayed approximately to the age of 24 weeks, and thus presenting a window for studying seeding-induced tau pathology. Seeding of tau pathology was induced by intrahippocampal injection of rTg4510 crude brain extracts (Fig. 4A). To determine the optimal time for the development of pathology, seeding was evaluated by AT8 immunohistochemistry (Fig. 4B, C) and Gallyas silver stain

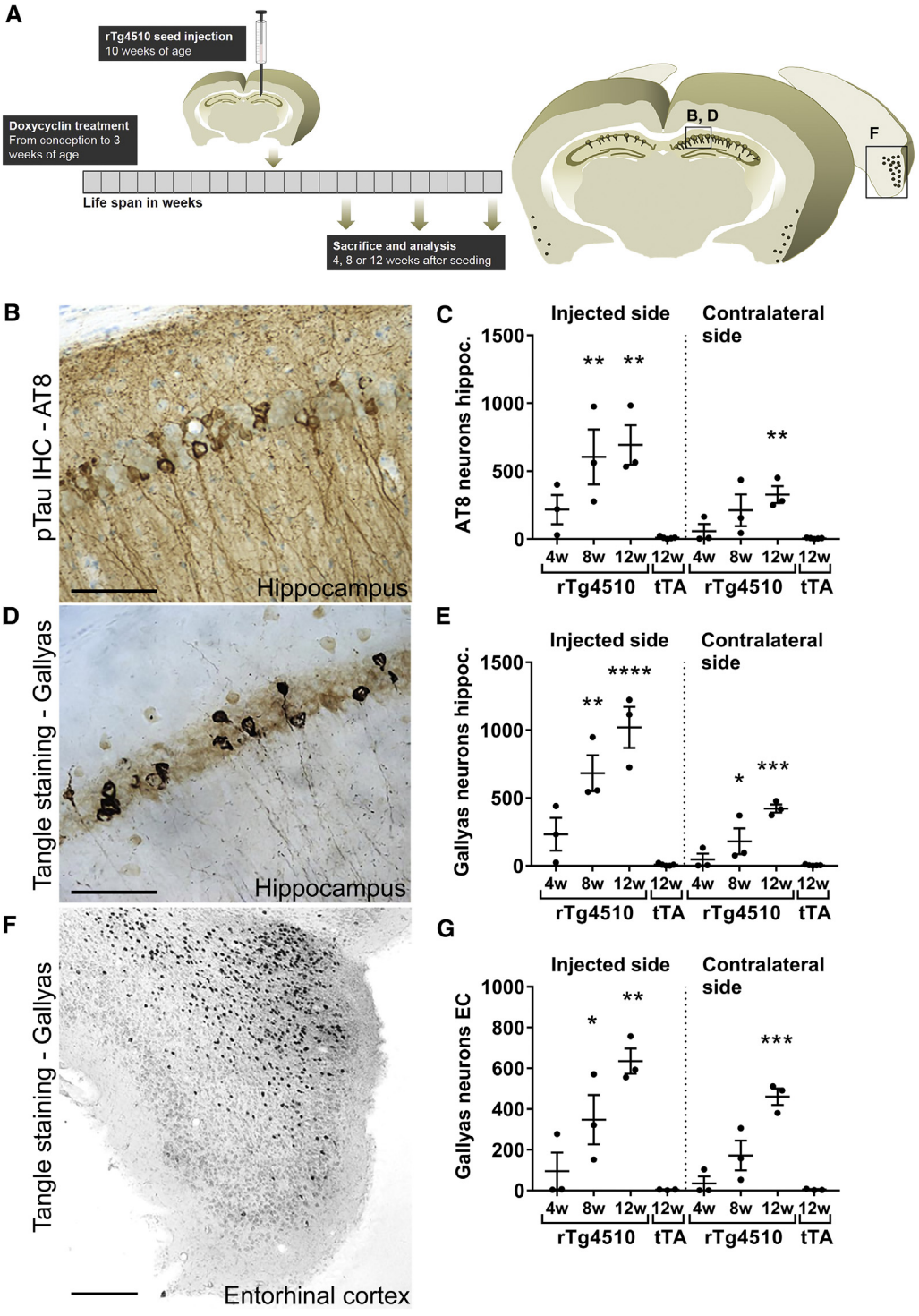

Fig. 4. Seeding model in rTg4510 mice. (A) Doxycycline-treated rTg4510 mice with delayed tau phosphorylation were unilaterally injected in hippocampus at age 10 weeks with crude extracts prepared from rTg4510 or tTA brains. Mice were housed for 4, 8, or 12 weeks and brains were processed for AT8 immunohistochemistry (B) to reveal phosphorylated tau; or the Gallyas silver stain (D, F) to reveal neurofibrillary tangles. Most seeded tau pathology developed bilaterally in the hippocampus and in the perirhinal and lateral entorhinal cortices. Scale bar in B and D: 50 μm and in F: 200 μm. (C, E) AT8- and Gallyas-positive neurons (soma) were counted on ipsilateral and contralateral sides of the hippocampus. Data represent accumulated number of positive neurons from eight coronal sections from each animal and mean ± SEM. (G) Gallyas-positive cells were quantified in the entorhinal cortex and data represent accumulated number of positive neurons from six coronal sections from each animal and mean ± SEM. N = 3 animals per time point. Nonparametric Kruskal-Wallis test and Dunn's multiple comparison test, $*P < .05$; $**P < .01$; $***P < .001$; $****P < .0001$. Abbreviation: SEM, standard error of the mean.

(Fig. 4D–G) 4, 8, and 12 weeks after seeding. Robust intracellular tau pathology developed in mice receiving rTg4510 extracts, whereas no or only limited pathology was observed in mice injected with control tTA extract (Fig. 4C, E, G). Tau pathology also developed in contralateral sides of hippocampus and lateral entorhinal cortex. Tau pathology increased over time and at 12 weeks there was a significant difference in the tangle load between mice injected with tTA and rTg4510 material in all regions quantified (Fig. 4C, E, G). At this time-point (i.e., at 22 weeks) we observed a weak AT8 signal in the hippocampus of rTg4510 mice receiving control tTA extracts (data not shown). This indicates that at this age, the overexpressed human tau begins to form detectable pretangles without the addition of seeds. Thus, we did not explore longer time-points and subsequently used the 12-week end point. This is in concordance to previous reports of other in vivo tau seeding models [9,11,37].

3.3.2. *Seeding with immunodepleted material*

We explored the role of specific tau species in vivo by performing tau seeding with rTg4510 and AD crude brain extracts depleted by either the D1.2 or the C10.2 antibody (as described in Section 3.1.4). Twelve weeks after injection with D1.2 or C10.2 depleted extracts only low levels of seeding were observed in the rTg4510 mouse (Fig. 5A, B). In contrast, by depletion of rTg4510 extract using the total tau antibody Tau5 (predominantly removing normal 55 kDa tau but only 20% of pS396-tau Supplementary Fig. 3A) the seeding activity was retained. We used Tau5 and C10.2 in combination to perform a maximal tau depletion; however, no additional reduction in seeding was observed (Fig. 5A).

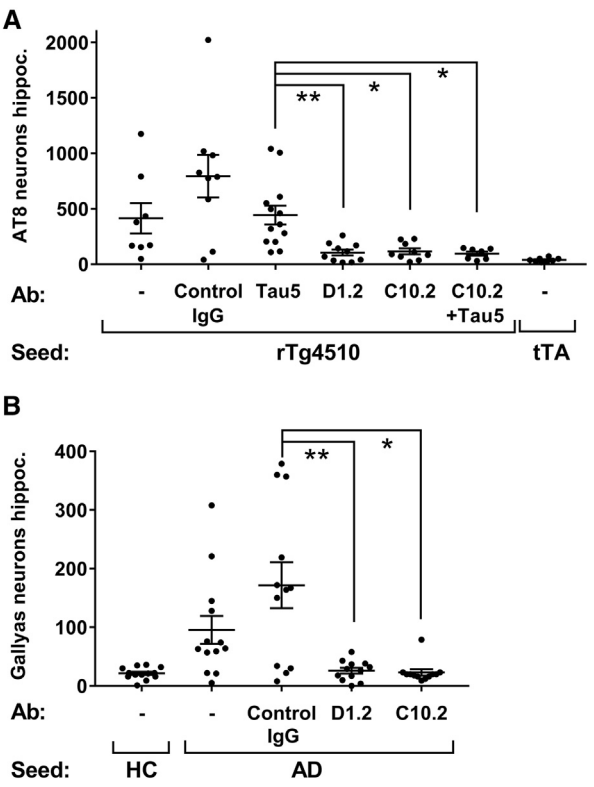

Fig. 5. In vivo seeding activity is reduced by depleting the rTg4510 and AD extracts with tau (p396) antibodies. Tau or control antibodies were used to immunodeplete crude extracts from (A) rTg4510 brains or (B) AD brains. The depleted extracts were injected unilaterally in hippocampus at age 10 and 12 weeks after injection, the number of AT8- or Gallyas-positive neurons was counted in the ipsilateral hippocampus. Data presented as accumulated number of positive neurons from eight sections from each animal and mean ± SEM, N = 7–10 (A) and N = 12–13 (B). Nonparametric Kruskal Wallis and Dunn's multiple comparison test, $*P < .05$; $**P < .01$. Abbreviations: AD, Alzheimer's disease; SEM, standard error of the mean.

3.3.3. *Effect of antibody treatment on seeding capacity*

Antibodies D1.2 and C10.2 were also evaluated in a therapeutic setting in rTg4510 mice seeded with rTg4510 crude extracts (Fig. 6A). The mice were dosed weekly with antibody (15 mg/kg, ip) for 14 weeks, starting 2 weeks before the seeding and continued until euthanized. Plasma levels of the antibodies were greater than 100 µg/mL at the time of seeding (data not shown). C10.2 treatment reduced the seeding by 74% ($P < .01$) and D1.2 treatment reduced the seeding by 66% ($P < .05$).

Furthermore, we explored the mechanism of inhibition by C10.2 in rTg4510 mice seeded with AD crude extracts by applying three different dosing paradigms (Fig. 6C). We compared dosing throughout (1) the entire seeding period (14 weeks, full), (2) start 4 weeks after seeding (post), and (3) C10.2 treatment only for 3 weeks, starting 2 weeks before injection (pre). Prevention of seeding and development of pathology was only observed when there was antibody (C10.2) exposure at the time of seed injection (full and pre) (Fig. 6D). Dosing of C10.2 4 weeks after seeding with AD brain material (post) had no effect. These data suggest that the antibody interacts with extracellular seeds and thereby prevents seeding and further development of tau pathology.

4. Discussion

The epitope defined by phosphorylation of S396 in tau has been heavily implicated in AD-associated tau pathology [38] and provides a valuable target for the development of therapeutic antibodies to capture tau and prevent spreading of tau pathology. Here, we describe the generation and characterization of such an antibody.

4.1. *pS396-tau-specific antibodies C10.2 and D1.2 selectively recognize pathologic tau in AD and rTg4510 brain material*

The binding of C10.2 and D1.2 to phospho-tau peptides (pS396) and (pS396/pS404) showed similar affinity (11–31 nM) indicating that both antibodies specifically recognize the pS396-tau epitope independently of the pS404 residue. Binding to in vitro phosphorylated tau-441 is also similar for C10.2 (IC_{50}; 104 pM) and D1.2 (IC_{50};

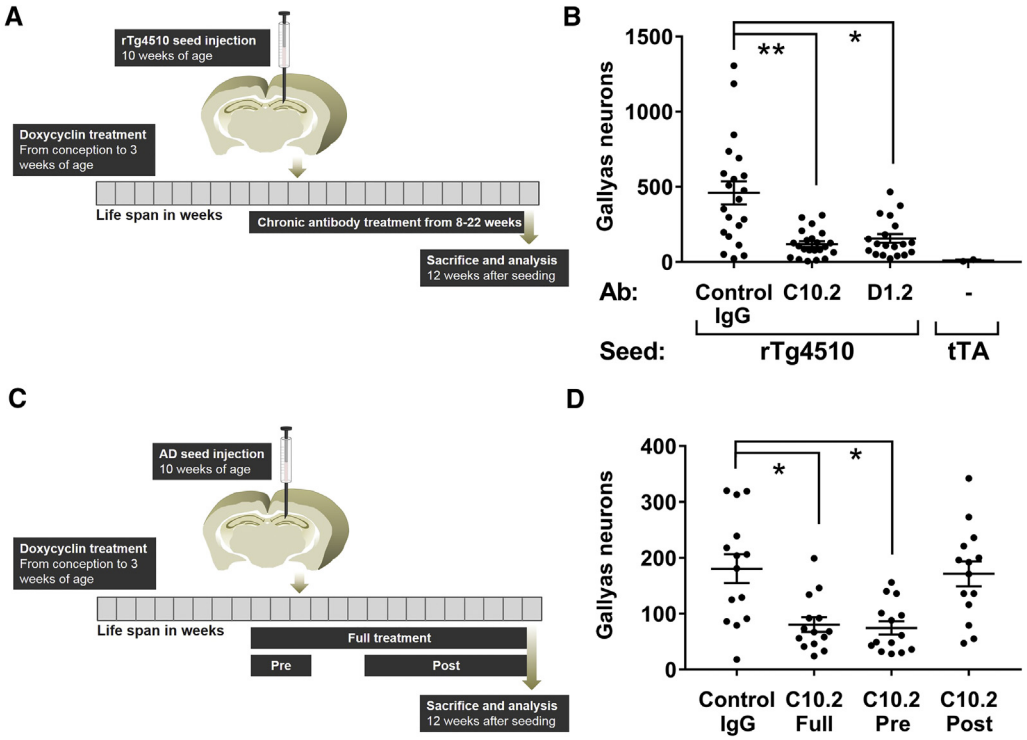

Fig. 6. C10.2 and D1.2 treatment decreases tau seeding in the rTg4510 model. (A, B) Mice were dosed once weekly with 15 mg/kg antibody beginning 2 weeks before hippocampal seeding with rTg4510 crude extracts. The treatment was continued until sacrifice at age 22 weeks. Gallyas-positive cells were quantified in the ipsilateral hippocampus revealing reduced tangle pathology by C10.2 (74%) and D1.2 (66%). (C, D) Different dosing paradigms were applied to the rTg4510 seeding model by C10.2-treatment before seeding (pre; 8–10 weeks old), after seeding (post; 14–22 weeks old), or full treatment at age from 8 to 22 weeks. In all groups, seeding was performed by injection of AD crude extract at age 10 weeks. Control IgG-treated mice served as positive controls. Data presented as accumulated number of positive neurons from eight sections from each animal and mean ± SEM, N = 20–22 for the rTg4510 injected groups and N = 2 for the tTa group (B) and N = 14 (D). Nonparametric Kruskal-Wallis and Dunn's multiple comparison test, $*P < .05$; $**P < .01$. Abbreviations: AD, Alzheimer's disease; IgG, immunoglobulin G; SEM, standard error of the mean.

50 pM). The higher affinity to phosphorylated tau-441 relative to the peptides may reflect a more efficient display of the antibody-binding epitope in the full-length tau. Both antibodies also recognize hyperphosphorylated tau in AD brain material in the immobilized phase (dot blot, Western blot). Notably, only C10.2 exhibits an effective binding in solution phase competition assays toward human AD P3 with an IC_{50} of 1.2 nM. This suggests that insoluble human AD tau (P3), when in solution phase, presents a conformation of the pS396 epitope recognized by C10.2 but not by D1.2. The binding mode of a pS396-tau–specific antibody in complex with a tau model-substrate peptide has been determined by x-ray crystallography [39]. This crystal structure demonstrates the antibody C5.2 (variant of antibody C10.2) binds to a unique extended conformation of the tau peptide chain, stabilized by an interaction between the Y394 and the pS396 side chains. The cryo-electron microscopy crystal structure of AD-generated MTB domains has been determined recently showing the β-sheet structure of the protofibrils [14]. The S396 epitope lies within the flanking region of the β-sheet structure and phosphorylation at S396 may stabilize this conformation.

The antibody C10.1 specifically recognizes the pS404 epitopes in tau peptides, but does not bind hyperphosphorylated tau isolated from rTg4510 and AD brains. Furthermore, C10.1 is not able to block seeding in HEK293 and neuronal in vitro assays, indicating that this antibody is not able to efficiently engage with tau seeding material. However, others have explored the therapeutic utility of targeting the pS404 epitope. Ittner et al. [29] conducted a passive immunotherapy study using presumed pS404-specific antibodies in two transgenic tau mouse models. They report a reduction in tau pathology after treatment with an IgG2a but not with an IgG1 isotype mouse antibody. This suggests that recruitment of microglia through antibody immune complexes plays a role for clearance of tau pathology by these tau antibodies.

4.2. Antibody C10.2 recognizes the in vitro seeding-competent pool of tau

C10.2 is differentiated from D1.2 and PHF13 antibodies by its ability to bind phosphorylated tau in the AD P3 solution phase competition assay, whereas the three antibodies show similar binding to in vitro phosphorylated tau. This

discrepancy in binding features between different pS396-specific antibodies suggests that there is a variation in the phospho-tau antigenic epitope display. Concurring with P3 solution phase competition binding data, C10.2 shows more efficient depletion in the pS396 bands in AD extracts compared with D1.2, when examined by Western blot analysis. In conjunction with this, D1.2 demonstrates limited anti-seeding effects in rTg4510 primary neurons and human tau-overexpressing HEK293 cells. Thus, we have demonstrated that the pool of tau recognized by C10.2 constitutes most of the in vitro seeding-competent tau observed in the human AD brain.

Earlier studies [13] identified small fibrils of hyperphosphorylated tau as the main seeding competent species in AD models. Although these species may be highly heterogeneous and composed of several proteolytically digested fragments of tau, it appears from the present study that C10.2 will recognize most of these tau species. Recent structural studies suggest that the folding core for the main seeding species in tau is constituted of the MTB domains (residues 306–378) [14]. This seeding core may not be fully accessible to antibodies in its aggregated form. For this reason, the optimal antibody for therapeutic intervention should recognize the more exposed MTB flanking regions, like C10.2.

4.3. pS396-tau antibodies prevent in vivo tau seeding

We used our rTg4510 model with delayed onset of tau pathology to explore anti-seeding properties of the antibodies. Our studies demonstrate that C10.2 and D1.2 antibodies effectively prevent the development of the tau pathology induced by injection of crude rTg4510 or AD brain extracts into the hippocampus. This was demonstrated both by immunodepletion and by systemic antibody treatment. The specific binding properties of C10.2 shown in the in vitro seeding models do not translate into superior in vivo efficacy over the D1.2 antibody. We attribute this to a much lower sensitivity of this model in comparison, that is, a higher load of seeding material was needed to obtain a measurable histologic readout. Furthermore, the in vivo studies were conducted with an excess of antibody, and breakdown of the blood-brain barrier during surgery may contribute to an increased local exposure. The predictive and translational value of these models remains to be demonstrated in clinical trials. Others have demonstrated that the pS396 targeting antibody PHF13 can reduce seeding in P301S mice (PS19) seeded with artificial MTB preformed tau fibrils (K18PL) [24]. In our study, PHF13 and D1.2 show similar binding profiles. Both bind full-length phosphorylated tau but not the AD P3 fraction in a solution phase assay.

We observe no evidence that the antibodies are independently taken up by neurons and elicit their action within the cell. However, we do observe that antibody-tau complexes are taken up by the primary neuronal cultures, as earlier demonstrated [31]. Thus, the effect on pathology observed in vivo may reflect inability of antibody-decorated brain extracts to induce seeding and aggregation in the host cell. This is supported by the observation that prevention is only possible when there is C10.2 exposure at the time of seed injection and not when the antibody is dosed after the tau seeds have been taken up. The role of active clearance mechanisms via microglia and astrocytes has not been investigated in this study.

The rTg4510 seeding model presented here demonstrates antibody-induced inhibition of tau seeding but not secondary propagation to other neurons. Endogenous phosphorylation of the human tau transgene in rTg4510 mice supersedes the time point where we can expect to detect an interneuronal spread of pathology. A longer interval than the 12 weeks that is achievable in the present model is likely required, as has been previously demonstrated [40].

4.4. Therapeutic potential

In light of failed clinical trials using small molecules to inhibit tau phosphorylation (glycogen synthase kinase 3 inhibitor [41]) or aggregation (leuco-methylthioninium bis [42]), immunotherapy targeting the propagation of tau pathology offers an attractive new endeavor to treat AD. Recent studies highlight differences in neutralization efficiency of tau seeds by a panel of antibodies, suggesting that not all tau epitopes present optimal targets for immunotherapy [30]. Seeding and spreading is believed to be an ongoing process in the AD brain and our data indicate that C10.2 would specifically target tau seeds and neutralize these when present in the extracellular space. A humanized mouse monoclonal antibody (based on C10.2) specifically targeting hyperphosphorylated tau has entered clinical development for the potential treatment of AD.

5. Conclusions

We have generated a murine monoclonal antibody, C10.2, that specifically recognizes the pS396 tau epitope and selectively binds AD and rTg4510 brain material. C10.2 exhibits unique solution phase binding properties in interaction with AD hyperphosphorylated tau. C10.2 potently prevents tau seeding in cellular and in vivo assays. To sum up, our studies suggest that C10.2 uniquely recognizes the pS396 epitope as it is presented in AD brains, and thus provides a promising candidate for immunotherapy.

Acknowledgments

The authors like to thank the following for substantial and excellent technical support: Lone Lind Hansen, Annette Bjørn, Karina Lynge, Bo Albrechtslund, Kirsten Assing, Anette Bredal Christiansen, Kirsten Jørgensen, and Pia Møller Carstensen.

Disclosures: N.R., A.A.A., J.F.P., L.H., C.V., L.Ø.P., S.C., F.K., C.R.A., F.S., J.E., J.T.P. are full time employees of

H. Lundbeck A/S, Valby, Denmark. The research presented in this study was fully funded by H. Lundbeck A/S.

Supplementary data

Supplementary data to this article can be found online at https://doi.org/10.1016/j.trci.2018.09.005.

RESEARCH IN CONTEXT

1. Systematic review: Hyperphosphorylated tau has been established as a hallmark of Alzheimer's disease (AD) in the scientific literature. Specific phosphorylation sites appear to be more frequently phosphorylated in hyperphosphorylated pathologic tau associated with disease.
2. Interpretation: Hyperphosphorylated tau forms a key seeding species in seeding and spreading of tau pathology in AD and other tauopathies. The heterogeneous pool of hyperphosphorylated tau can be targeted with phospho-tau specific monoclonal antibodies. Phospho-serine 396 (pS396) specific anti-tau antibodies have been generated, which target the complete heterogeneous pool of hyperphosphorylated tau.
3. Future directions: A humanized version of one of these antibodies (C10.2) will soon enter into clinical trials for the treatment of AD.

References

[1] Lee VM, Goedert M, Trojanowski JQ. Neurodegenerative tauopathies. Annu Rev Neurosci 2001;24:1121–59.
[2] Greenberg SG, Davies P. A preparation of Alzheimer paired helical filaments that displays distinct tau proteins by polyacrylamide gel electrophoresis. Proc Natl Acad Sci U S A 1990;87:5827–31.
[3] Hanger DP, Anderton BH, Noble W. Tau phosphorylation: the therapeutic challenge for neurodegenerative disease. Trends Mol Med 2009;15:112–9.
[4] Kanemaru K, Takio K, Miura R, Titani K, Ihara Y. Fetal-type phosphorylation of the tau in paired helical filaments. J Neurochem 1992;58:1667–75.
[5] Kopke E, Tung YC, Shaikh S, Alonso AC, Iqbal K, Grundke-Iqbal I. Microtubule-associated protein tau. abnormal phosphorylation of a non-paired helical filament pool in Alzheimer disease. J Biol Chem 1993;268:24374–84.
[6] Braak H, Braak E. Demonstration of amyloid deposits and neurofibrillary changes in whole brain sections. Brain Pathol 1991;1:213–6.
[7] Nelson PT, Alafuzoff I, Bigio EH, Bouras C, Braak H, Cairns NJ, et al. Correlation of Alzheimer disease neuropathologic changes with cognitive status: a review of the literature. J Neuropathol Exp Neurol 2012;71:362–81.
[8] Braak H, Braak E, Strothjohann M. Abnormally phosphorylated tau protein related to the formation of neurofibrillary tangles and neuropil threads in the cerebral cortex of sheep and goat. Neurosci Lett 1994;171:1–4.
[9] Clavaguera F, Bolmont T, Crowther RA, Abramowski D, Frank S, Probst A, et al. Transmission and spreading of tauopathy in transgenic mouse brain. Nat Cell Biol 2009;11:909–13.
[10] Clavaguera F, Hench J, Lavenir I, Schweighauser G, Frank S, Goedert M, et al. Peripheral administration of tau aggregates triggers intracerebral tauopathy in transgenic mice. Acta Neuropathol 2014;127:299–301.
[11] Ahmed Z, Cooper J, Murray TK, Garn K, McNaughton E, Clarke H, et al. A novel in vivo model of tau propagation with rapid and progressive neurofibrillary tangle pathology: the pattern of spread is determined by connectivity, not proximity. Acta Neuropathol 2014;127:667–83.
[12] Falcon B, Cavallini A, Angers R, Glover S, Murray TK, Barnham L, et al. Conformation determines the seeding potencies of native and recombinant Tau aggregates. J Biol Chem 2015;290:1049–65.
[13] Jackson SJ, Kerridge C, Cooper J, Cavallini A, Falcon B, Cella CV, et al. Short fibrils constitute the major species of seed-competent tau in the brains of mice transgenic for human P301S tau. J Neurosci 2016;36:762–72.
[14] Fitzpatrick AWP, Falcon B, He S, Murzin AG, Murshudov G, Garringer HJ, et al. Cryo-EM structures of tau filaments from Alzheimer's disease. Nature 2017;547:185–90.
[15] Asuni AA, Boutajangout A, Quartermain D, Sigurdsson EM. Immunotherapy targeting pathological tau conformers in a tangle mouse model reduces brain pathology with associated functional improvements. J Neurosci 2007;27:9115–29.
[16] Theunis C, Crespo-Biel N, Gafner V, Pihlgren M, Lopez-Deber MP, Reis P, et al. Efficacy and safety of a liposome-based vaccine against protein tau, assessed in tau.P301L mice that model tauopathy. PLoS One 2013;8:e72301.
[17] Boutajangout A, Quartermain D, Sigurdsson EM. Immunotherapy targeting pathological tau prevents cognitive decline in a new tangle mouse model. J Neurosci 2010;30:16559–66.
[18] Bi M, Ittner A, Ke YD, Gotz J, Ittner LM. Tau-targeted immunization impedes progression of neurofibrillary histopathology in aged P301L tau transgenic mice. PLoS One 2011;6:e26860.
[19] Boimel M, Grigoriadis N, Lourbopoulos A, Haber E, Abramsky O, Rosenmann H. Efficacy and safety of immunization with phosphorylated tau against neurofibrillary tangles in mice. Exp Neurol 2010;224:472–85.
[20] Troquier L, Caillierez R, Burnouf S, Fernandez-Gomez FJ, Grosjean ME, Zommer N, et al. Targeting phospho-Ser422 by active Tau immunotherapy in the THYTau22 mouse model: a suitable therapeutic approach. Curr Alzheimer Res 2012;9:397–405.
[21] Yanamandra K, Kfoury N, Jiang H, Mahan TE, Ma S, Maloney SE, et al. Anti-tau antibodies that block tau aggregate seeding in vitro markedly decrease pathology and improve cognition in vivo. Neuron 2013;80:402–14.
[22] Boutajangout A, Ingadottir J, Davies P, Sigurdsson EM. Passive immunization targeting pathological phospho-tau protein in a mouse model reduces functional decline and clears tau aggregates from the brain. J Neurochem 2011;118:658–67.
[23] Chai X, Wu S, Murray TK, Kinley R, Cella CV, Sims H, et al. Passive immunization with anti-Tau antibodies in two transgenic models: reduction of Tau pathology and delay of disease progression. J Biol Chem 2011;286:34457–67.
[24] Sankaranarayanan S, Barten DM, Vana L, Devidze N, Yang L, Cadelina G, et al. Passive immunization with phospho-tau antibodies reduces tau pathology and functional deficits in two distinct mouse tauopathy models. PLoS One 2015;10:e0125614.
[25] Collin L, Bohrmann B, Gopfert U, Oroszlan-Szovik K, Ozmen L, Gruninger F. Neuronal uptake of tau/pS422 antibody and reduced

progression of tau pathology in a mouse model of Alzheimer's disease. Brain 2014;137:2834–46.
[26] D'Abramo C, Acker CM, Jimenez HT, Davies P. Tau passive immunotherapy in mutant P301L mice: antibody affinity versus specificity. PLoS One 2013;8:e62402.
[27] Dai CL, Hu W, Tung YC, Liu F, Gong CX, Iqbal K. Tau passive immunization blocks seeding and spread of Alzheimer hyperphosphorylated Tau-induced pathology in 3 x Tg-AD mice. Alzheimers Res Ther 2018;10:13.
[28] Castillo-Carranza DL, Sengupta U, Guerrero-Munoz MJ, Lasagna-Reeves CA, Gerson JE, Singh G, et al. Passive immunization with Tau oligomer monoclonal antibody reverses tauopathy phenotypes without affecting hyperphosphorylated neurofibrillary tangles. J Neurosci 2014;34:4260–72.
[29] Ittner A, Bertz J, Suh LS, Stevens CH, Gotz J, Ittner LM. Tau-targeting passive immunization modulates aspects of pathology in tau transgenic mice. J Neurochem 2015;132:135–45.
[30] Vandermeeren M, Borgers M, Van Kolen K, Theunis C, Vasconcelos B, Bottelbergs A, et al. Anti-Tau monoclonal antibodies derived from soluble and filamentous tau show diverse functional properties in vitro and in vivo. J Alzheimers Dis 2018;65:265–81.
[31] Yanamandra K, Jiang H, Mahan TE, Maloney SE, Wozniak DF, Diamond MI, et al. Anti-tau antibody reduces insoluble tau and decreases brain atrophy. Ann Clin Transl Neurol 2015;2:278–88.
[32] Crowe A, Ksiezak-Reding H, Liu WK, Dickson DW, Yen SH. The N terminal region of human tau is present in Alzheimer's disease protein A68 and is incorporated into paired helical filaments. Am J Pathol 1991;139:1463–70.
[33] Santacruz K, Lewis J, Spires T, Paulson J, Kotilinek L, Ingelsson M, et al. Tau suppression in a neurodegenerative mouse model improves memory function. Science 2005;309:476–81.
[34] Helboe L, Egebjerg J, Barkholt P, Volbracht C. Early depletion of CA1 neurons and late neurodegeneration in a mouse tauopathy model. Brain Res 2017;1665:22–35.
[35] Sahara N, DeTure M, Ren Y, Ebrahim AS, Kang D, Knight J, et al. Characteristics of TBS-extractable hyperphosphorylated tau species: aggregation intermediates in rTg4510 mouse brain. J Alzheimers Dis 2013;33:249–63.
[36] Volbracht C, Penzkofer S, Mansson D, Christensen KV, Fog K, Schildknecht S, et al. Measurement of cellular beta-site of APP cleaving enzyme 1 activity and its modulation in neuronal assay systems. Anal Biochem 2009;387:208–20.
[37] Peeraer E, Bottelbergs A, Van Kolen K, Stancu IC, Vasconcelos B, Mahieu M, et al. Intracerebral injection of preformed synthetic tau fibrils initiates widespread tauopathy and neuronal loss in the brains of tau transgenic mice. Neurobiol Dis 2015;73:83–95.
[38] Bramblett GT, Goedert M, Jakes R, Merrick SE, Trojanowski JQ, Lee VM. Abnormal tau phosphorylation at Ser396 in Alzheimer's disease recapitulates development and contributes to reduced microtubule binding. Neuron 1993;10:1089–99.
[39] Chukwu JE, Pedersen JT, Pedersen LO, Volbracht C, Sigurdsson EM, Kong XP. Tau antibody structure reveals a molecular switch defining a pathological conformation of the tau protein. Sci Rep 2018;8:6209.
[40] de Calignon A, Polydoro M, Suarez-Calvet M, William C, Adamowicz DH, Kopeikina KJ, et al. Propagation of tau pathology in a model of early Alzheimer's disease. Neuron 2012;73:685–97.
[41] Lovestone S, Boada M, Dubois B, Hull M, Rinne JO, Huppertz HJ, et al. A phase II trial of tideglusib in Alzheimer's disease. J Alzheimers Dis 2015;45:75–88.
[42] Gauthier S, Feldman HH, Schneider LS, Wilcock GK, Frisoni GB, Hardlund JH, et al. Efficacy and safety of tau-aggregation inhibitor therapy in patients with mild or moderate Alzheimer's disease: a randomised, controlled, double-blind, parallel-arm, phase 3 trial. Lancet 2016;388:2873–84.